

Collaborative Representation for SPD Matrices with Application to Image-Set Classification

Li Chu, Rui Wang, and Xiao-Jun Wu*

Abstract—Collaborative representation-based classification (CRC) has demonstrated remarkable progress in the past few years because of its closed-form analytical solutions. However, the existing CRC methods are incapable of processing the nonlinear variational information directly. Recent advances illustrate that how to effectively model these nonlinear variational information and learn invariant representations is an open challenge in the community of computer vision and pattern recognition. To this end, we try to design a new algorithm to handle this problem. Firstly, the second-order statistic, i.e., covariance matrix is applied to model the original image sets. Due to the space formed by a set of nonsingular covariance matrices is a well-known Symmetric Positive Definite (SPD) manifold, generalising the Euclidean collaborative representation to the SPD manifold is not an easy task. Then, we devise two strategies to cope with this issue. One attempts to embed the SPD manifold-valued data representations into an associated tangent space via the matrix logarithm map. Another is to embed them into a Reproducing Kernel Hilbert Space (RKHS) by utilizing the Riemannian kernel function. After these two treatments, CRC is applicable to the SPD manifold-valued features. The evaluations on four benchmarking datasets justify its effectiveness.

Index Terms—Collaborative representation based classification, Symmetric positive definite matrix, Tangent space, Riemannian kernel space, Image set classification.

I. INTRODUCTION

Sparse representation based classification (SRC) has recently attracted increasing attention in the domain of digital image processing and pattern recognition due to its robustness [1]–[9]. It finds a sparse representation of the testing sample over the dictionary with sparsity constraints computed by minimizing the L_1 -norm based reconstruction error. Based on this, many papers explore innovative applications or design more discriminative dictionary learning models to further improve the visual classification performance [2], [10], [11]. Recently, some works have shown that collaborative representation is more efficient than L_1 -norm based sparsity constraint. To this end, Zhang et al. [12] propose a collaborative representation based classification (CRC) method using the L_2 -norm based regularization, and the experimental results show that CRC is able to achieve competitive classification performance but with lower computational complexity than SRC. Hence, CRC has attracted much attention due to its effectiveness [13]–[15].

However, the existing collaborative representation methods are mainly designed for Euclidean visual data, which can not encode the nonlinear variational information between image sets efficiently. Recently, image set classification has been proven to be an area of increasing vitality in the computer vision and pattern recognition community [16]–[25]. Compared to single-shot image-based classification [26]–[31], each image set generally contains a large number of images that belong to the same class and cover large variations such as pose changes, illumination differences and partial occlusions. When referring to the mathematical models of image set data, covariance matrix [32]–[34], linear subspace [35]–[37] and Gaussian distribution [38] are three well-known representation methods, among which, covariance matrices provide a natural data representation by computing the second-order statistic of a group of samples. Thus, we select it to describe each image set in this paper. According to the previous works [16], [22], [32], we know that the space formed by a family of covariance matrices with the same dimensionality is a non-linear Riemannian manifold. Specifically, it is an SPD manifold. As a consequence, the Euclidean learning approaches can not be applied to the SPD manifold-valued data directly. To handle this problem, some distance metrics have been developed on the Riemannian manifold for similarity measurement, such as Log-Euclidean Metric (LEM) [39] and Affine-Invariant Riemannian Metric (AIRM) [40]. By making use of these Riemannian metrics, the Euclidean computations can be generalized to the non-Euclidean data representations according to the following tactics.

Inspired by the superiority of kernel representation [41], the first type of tactic is to embed the original Riemannian manifold into a Reproducing Kernel Hilbert Space (RKHS) via Riemannian kernel functions [32], [35], [42], [43]. Although these methods can achieved favourable performance on several visual classification tasks, the Riemannian geometrical structure of the original set data may be distorted in the process of RKHS transformation. To solve this issue, some algorithms have been put forward to jointly perform similarity metric learning and embedding mapping learning on the original Riemannian manifolds directly. Accordingly, a lower-dimensional and more discriminative subspace can be generated for image set classification. Compared with the aforementioned strategy, this type of approach takes the Riemannian geometry of the original data manifold into fully consideration in the dimensionality reduction process, thus may lead to impressive classification performance. As a matter of fact, the methods mentioned above just model each given image set from a single geometrical perspective, which may

L. Chu, R. Wang, and X.-J. Wu (*Corresponding author*) are with the School of Artificial Intelligence and Computer Science, Jiangnan University, Wuxi 214122, China. L. Chu, R. Wang, and X.-J. Wu are also with Jiangsu Provincial Engineering Laboratory of Pattern Recognition and Computational Intelligence, Jiangnan University e-mail: (15861899728@163.com; cs_wr@jiangnan.edu.cn; xiaojun_wu_jnu@163.com).

lose some useful structural information for visual data. As a countermeasure, Wang et al. [23] and Huang et al. [44] utilize the metric learning method to learn an effective metric space for the heterogeneous features extracted from the multiple Riemannian manifold-valued descriptors.

In parallel with the above developments, sparse representation methods have received widespread attention in the context of Riemannian manifold due to its simplicity and striking performance [42], [45]–[48]. Obviously, these methods make use of sparse representation to perform representation learning, and L_1 -norm based sparsity usually leads to higher computational cost. Since the efficient L_2 -norm based collaborative representation has already shown its discriminatory power and higher computational efficiency, it is valuable to study whether CRC can also perform well on the SPD manifold. This study is planned for proposing the first attempt in this domain. With this objective, we present a collaborative representation-based image set classification in the scenario of SPD manifold in this paper. Fig. 1 indicates the basic idea of traditional Euclidean-based CRC and our approach. Compared with the Euclidean-based CRC (the top line of Fig. 1), we use the covariance matrix to model each image set. Generally speaking, the space formed by a set of covariance matrices is not a vector space but instead adhering to an SPD manifold. In order to make the collaborative representation applicable to the SPD manifold, we offer two strategies. The first strategy is to embed the original SPD manifold into an associated tangent space via matrix logarithm map (we use Log_CRC to represent this method). Another strategy is to exploit the Riemannian kernel function to map the original SPD manifold into RKHS (we call this method LogEK_CRC). In these two cases, the collaborative representation can be applied to conduct further feature learning and classification. The evaluations on four different benchmarking datasets verify the effectiveness of the proposed method.

II. RELATED WORKS

The existing Riemannian manifold-based image set classification methods can be grouped into four categories, such as Riemannian kernel-based discriminative learning methods [32], [35], [37], [42], [43], Riemannian manifold dimensionality reduction methods [16], [33], [34], [36], multiple statistics fusion-based methods [23], [44], and Riemannian manifold-based sparse representation methods [42], [45]–[48]. The working mechanism of the first type of approach is to embed the original Riemannian manifold into a Reproducing Kernel Hilbert Space (RKHS) via Riemannian kernel functions [32], [35], [42], [43]. Therein, Wang et al. [32] derive a Log-Euclidean Metric-based kernel function to transform the original SPD manifold into RKHS. Similarly, Hamm et al. [35] embed the original Grassmann manifold into RKHS via the projection kernel function. Besides, both [32] and [35] utilize the kernel discriminant analysis algorithm to perform discriminant subspace learning. In order to improve the description ability of the Riemannian kernel-based approach, Wang et al. [?] first builds a lightweight feature extraction network on the original Grassmann manifold for the sake of learning

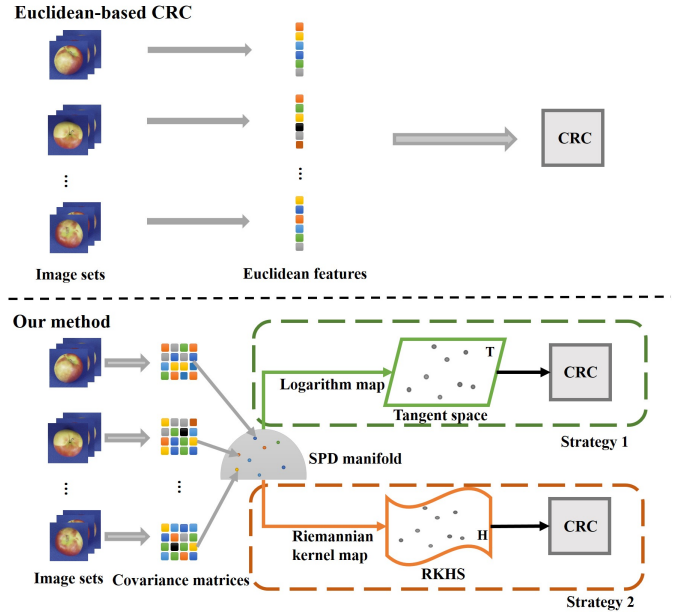


Fig. 1: Overview of the Euclidean-based CRC and our method. Euclidean-based CRC: Each image set is described as a vector feature. Our method: Each image set is represented by a covariance matrix which resides on the SPD manifold. To make collaborative representation work for the manifold-value data, we provide two strategies, one is to embed the SPD manifold into a tangent space via matrix logarithm map (Strategy 1 in the figure). Another transforms the SPD manifold to RKHS by exploiting Riemannian kernel function (Strategy 2 in the figure).

fine-grained geometric features, Then, the projection kernel function is applied to map the generated data representations into the kernel space for the subsequent metric learning process. However, one shortcoming of this type of approach is that the Riemannian geometrical structure of the original set data may be changed in the feature transformation process.

To solve this problem, a slice of algorithms have been proposed to jointly perform similarity metric learning and embedding mapping learning on the original Riemannian manifolds directly. Wherein, Harandi et al. [34] propose to model the orthonormal mapping from the original high-dimensional SPD manifold to a lower-dimensional one with a metric learning framework. Similarly, Huang et al. [36] construct a metric learning framework on the original Grassmann manifold for the purpose of directly yielding a lower-dimensional and more appropriate Grassmann manifold for classification. Differently, Huang et al. [16] propose a novel Log-Euclidean metric learning framework on the SPD manifold tangent space, which can not only produce a desirable new SPD manifold, but also demonstrate higher computational efficiency. As a matter of fact, the aforementioned approaches just model each given image set from a single geometrical perspective, which may lose some useful structural information for visual classification. Therefore, Wang et al. [23] and Huang et al. [44] propose to model each given image set with different visual statistics simultaneously. Since different statistics reside

in different topological spaces, the metric learning framework is designed to fuse these hybrid features into a unified subspace for improved classification.

In parallel with the above developments, the Riemannian manifold-based sparse representation methods have obtained widespread attention due to its simplicity and efficiency in representation learning [42], [45]–[48]. Therein, Kai et al. [45] propose to embed the original SPD manifold-valued data into an associated tangent space via matrix logarithm map. In this case, the existing sparse representation methods apply. Different from [45], Harandi et al. [42] utilize the Stein kernel to embed the original SPD manifold-valued features into RKHS. Consequently, the sparse representation also can be carried out in it. Similarly, Li et al. [47] and Harandi et al. [48] try to generalise the sparse representation to the Riemannian manifolds by exploiting the Log-Euclidean kernel and Jeffrey kernel, respectively.

III. BACKGROUND THEORY

Before introducing our method, we briefly review the covariance matrix, tangent space, and Riemannian kernel function, respectively.

A. Covariance matrix

Let $S_i = \{s_1, s_2, \dots, s_{n_i}\}$ be an image set with n_i images, where $s_i \in \mathbb{R}^d$ is the i -th vectorized instance. We model the image set S_i as the $d \times d$ covariance matrix [32], [33], [34]:

$$X = \frac{1}{n-1} \sum_{i=1}^n (s_i - u_{S_i})(s_i - u_{S_i})^T \quad (1)$$

where u_{S_i} is the mean of S_i . In order to prevent covariance matrix from being singular, we add a small perturbation value to X : $\hat{X} \leftarrow X + \lambda I$, where λ is set to $10^{-3} \times \text{trace}(C)$ and I is the identity matrix [32].

B. Tangent space and Riemannian kernel function

The covariance matrix X computed by Eq.(1) does not lie in a vector space but instead adhering to a nonlinear Riemannian manifold, i.e., SPD manifold Sym_d^+ . As a consequence, the Euclidean computations are inapplicable. Arsigny et al. [49] propose to use the matrix logarithm map to transform the manifold of covariance matrices into a vector space of symmetric matrices. Let $X = U\Sigma U^T$ be the eigen-decomposition of covariance matrix X , where Σ is the diagonal matrix of eigenvalues, U is the corresponding eigenvectors matrix. Then, the matrix logarithm map can be expressed as

$$\log(X) = U \log(\Sigma) U^T \quad (2)$$

where $\log(\Sigma)$ is the diagonal matrix of the eigenvalue logarithms.

When it comes to similarity measurement on SPD manifold, Log-Euclidean Metric(LEM) [39] is a widely used distance measure, which corresponds to an Euclidean metric in the logarithmic domain. The distance between two points X_i, X_j on Sym_d^+ is computed by LEM as:

$$d_{LEM}(X_i, X_j) = \|\log(X_i) - \log(X_j)\|_F \quad (3)$$

where $\|\cdot\|_F$ means the matrix Frobenius norm.

Under this metric, a Riemannian kernel [47] can be formulated as:

$$k(X_i, X_j) = \exp\left(-\beta \|\log(X_i) - \log(X_j)\|_F^2\right) \quad (4)$$

the validity of which has been confirmed in [47].

IV. COLLABORATIVE REPRESENTATION FOR SPD MATRICES

This section minutely presents the proposed collaborative representation method for SPD matrices. Specifically, Section A discusses the strategic details of mapping the SPD manifold into an associated tangent space, and we introduce the collaborative representation in RKHS in Section B. Let $\tilde{S} = \{S_1, S_2, \dots, S_N\}$ be the gallery composed by N image sets, with each set expressed as: $S_i = \{s_1, s_2, \dots, s_{n_i}\} \in \mathbb{R}^{d \times n_i}$, where $i = 1 \rightarrow N$, and n_i means the number of images in the i -th image set, S_i belongs to category c_i . From the previous studies [32], [33], [34], we know that each image set can be represented by a covariance matrix in Eq.(1). Then, we use $\tilde{X} = \{X_1, X_2, \dots, X_N\}$ to denote the computed SPD manifold-valued feature representations of the gallery \tilde{S} .

A. Collaborative representation in tangent space(Log_CRC)

Collaborative representation has been proven to have a good performance for Euclidean data. But, it can not be applied to the SPD manifold-valued features directly. To address this problem, we embed each sample of \tilde{X} into the tangent space by using the logarithm map $\Psi_{\log} : Sym_d^+ \rightarrow T$, where T means the associated tangent space of \tilde{X} . And the points in the tangent space are expressed as $L_X = \{L_1, L_2, \dots, L_N\}$, $L_i = \log(X_i) \in \mathbb{R}^{d \times d}$. To facilitate the subsequent computations, we further convert each tangent map into a vector. $l_X = \{l_1, l_2, \dots, l_N\}$ is used to denote the vectorized matrix of L_X and $l_i = \text{vec}(L_i) \in \mathbb{R}^{d^2}$. Similarly, we can use the same procedure to obtain the vectorized query set. For each query data y , it can be collaboratively represented as l_X and classified by measuring which class leads to the minimum reconstruction error. The representation vector w is obtained by solving the following objective function:

$$w = \min \left\{ \|y - l_X w\|_2^2 + \lambda_1 \|w\|_2 \right\} \quad (5)$$

where λ_1 is the regularization parameter.

The solution to Eq.5 can be easily derived as:

$$w = (l_X^T l_X + \lambda_1 I)^{-1} l_X^T y \quad (6)$$

where I is an identity matrix. The reconstruction error between the query sample y and the gallery with respect to class c is

$$Err_c = \|y - l_X^c w_c\|_2 / \|w_c\|_2 \quad (7)$$

where l_X^c denotes the data collected by l_X from the c -th class and w_c is the corresponding collaborative representation coefficients with respect to class c , y is assigned to the class with the smallest reconstruction error

$$\text{label} = \min_c (Err_c), c = 1, 2, \dots, k \quad (8)$$

where k indicates the number of classes.

Algorithm: The proposed method

Input:

- The gallery: $\tilde{X} = \{X_1, X_2, \dots, X_N\}$, $X_i \in Sym_d^+$
- The regularization parameter: λ_1, λ_2

Output:

- Class label
-

Log_CRC method:

1: Get the tangent space data $L_X = \{L_1, L_2, \dots, L_N\}$ by logarithm map in Eq.(2).

2: Obtain the vectorized data in the tangent space: $l_X = \{l_1, l_2, \dots, l_N\}$.

3: Compute the collaborative representation coefficient for each vectorized test point y via:

$$w = (l_X^T l_X + \lambda_1 I)^{-1} l_X^T y.$$

4: Compute the reconstruction error of y and the data for class c via $Err_c = \|y - l_X^c w_c\|_2 / \|w_c\|_2$.

5: Get the class label by $\min_c (Err_c)$, $c = 1, 2, \dots, k$.

LogEK_CRC method:

1: Compute the $K_{\tilde{X}\tilde{X}}$, $K_{\tilde{X}Y}$ and K_{YY} by Riemannian kernel function in Eq.(4).

2: Perform SVD on $K_{\tilde{X}\tilde{X}} = U\Sigma U^T$.

2: Compute $\Psi = (U\Sigma^{1/2})^T$ in Eq.(11) and then get $\Phi = (\Psi^T)^{-1} K_{\tilde{X}Y}$.

4: Get the collaborative representation coefficient for each query point $Y \in Sym_d^+$ via:

$$w = (\Psi^T \Psi + \lambda_2 I)^{-1} \Psi^T \Phi.$$

5: Compute $\min_c \{\|\Phi - \Psi_c w_c\|_2 / \|w_c\|_2\}$ to get the class label of \tilde{Y} .

B. Collaborative representation in RKHS(LogEK_CRC)

To make the Euclidean collaborative representation applicable to the SPD manifold-valued data, another strategy is to transform the SPD manifold to RKHS by employing the Riemannian kernel function specified in Eq. 4. This mapping process is expressed as: $\phi : Sym_d^+ \rightarrow H$. We use $\phi(\tilde{X}) = \{\phi(X_1), \phi(X_2), \dots, \phi(X_N)\}$ to represent the new feature representation of \tilde{X} in Riemannian kernel space H . For each query point Y on Sym_d^+ , the Riemannian kernel collaborative representation [50] in the RKHS is formulated as:

$$w = \min \left\{ \left\| \phi(Y) - \phi(\tilde{X})w \right\|_2^2 + \lambda_2 \|w\|_2^2 \right\} \quad (9)$$

where λ_2 is the regularization parameter. According to Mercer theorem [51], the inner product between two points in kernel space can be represented by their kernel function $k(X_i, X_j) = \langle \phi(X_i), \phi(X_j) \rangle$. With the Riemannian kernel defined in Eq.(4), Eq.(9) is expanded as

$$K_{YY} - 2w^T K_{\tilde{X}Y} + w^T K_{\tilde{X}\tilde{X}} w + \lambda_2 \|w\|_2^2 \quad (10)$$

where, $K_{\tilde{X}\tilde{X}}$ is a $N \times N$ matrix, each element of the matrix describes the similarity between data in the gallery,

i.e., $k(X_i, X_j)$, where $i = 1, 2, \dots, N$ and $j = 1, 2, \dots, N$. $K_{\tilde{X}Y}$ is a $N \times 1$ vector which consists of $k(X_i, Y)$, $i = 1, 2, \dots, N$.

Inspired by [52], in order to further simplify Eq.(10), the matrix $K_{\tilde{X}\tilde{X}}$ is rewritten through Singular Value Decomposition (SVD)

$$K_{\tilde{X}\tilde{X}} = U\Sigma U^T = U\Sigma^{1/2} (\Sigma^{1/2})^T U^T = \Psi^T \Psi \quad (11)$$

where Σ is the diagonal matrix of eigenvalues, U is the corresponding eigenvectors matrix. $\Psi = (U\Sigma^{1/2})^T$ is the approximate representation of \tilde{X} in Riemannian kernel space, i.e., $\phi(\tilde{X})$. Further, $K_{\tilde{X}Y}$ can be rewritten as

$$K_{\tilde{X}Y} = \Psi^T (\Psi^T)^{-1} K_{\tilde{X}Y} = \Psi^T \Phi \quad (12)$$

where $\Phi = (\Psi^T)^{-1} K_{\tilde{X}Y}$ is the approximate representation of Y in Riemannian kernel space, i.e., $\phi(Y)$. Similarly, $K_{YY} = \Phi^T \Phi$. Thus, we get

$$\begin{aligned} & \Phi^T \Phi - 2w^T \Psi^T \Phi + w^T \Psi^T \Psi w + \lambda_2 \|w\|_2^2 \\ & = \|\Phi - \Psi w\|_2^2 + \lambda_2 \|w\|_2^2 \end{aligned} \quad (13)$$

w can be derived as

$$w = (\Psi^T \Psi + \lambda_2 I)^{-1} \Psi^T \Phi \quad (14)$$

then we obtain the label of Y

$$\begin{aligned} \text{label} &= \min_c \left\{ \left\| \phi(Y) - \phi(\tilde{X})_c w_c \right\|_2 / \|w_c\|_2 \right\} \\ &= \min_c \left\{ \|\Phi - \Psi_c w_c\|_2 / \|w_c\|_2 \right\} \\ &c = 1, 2, \dots, k \end{aligned} \quad (15)$$

where Ψ_c is the data associated with the c -th class, w_c is the collaborative representation coefficients with respect to class c , k indicates the number of classes.

C. Relation With the Previous Works

The proposed approach is related to two previous works [53], [54]. In this part, we summarize some essential differences between our method and those introduced in [53] and [54] in the following two paragraphs.

Relation With [53]. In fact, both the proposed algorithm and [53] try to generalise the Euclidean collaborative representation to the Riemannian manifold-valued feature representations for the sake of improving the image set classification performance on some challenging visual scenarios. However, there exist some fundamental differences among them: 1) for feature representation, the proposed approach is executed in the scenario of SPD manifold, while [53] is carried out in the context of Grassmann manifold; 2) based on the generated Grassmann manifold-valued features, [53] constructs the $P+V$ model to encode the inter-class similarity information and the intra-class variational information of the data, while the proposed approach does not consider this explicitly; 3) with the constructed $P+V$ model, [53] implements the collaborative representation framework with prototype learning in the space spanned by a set of symmetric matrices. As a result, the dictionary learning problem could be converted into standard Euclidean problem. Different from [53], our method implements it in two ways. The first is to map the original SPD

manifold into an associated tangent space, and the second is to embed it into the RKHS. Since both the tangent space and the RKHS conform to the Euclidean geometry, the collaborative representation applies.

Relation With [54]. Actually, both the proposed algorithm and [54] devote to extend the traditional single image-based collaborative representation to the image set-based one to inject new vigour for image set classification. But, they demonstrate different representation learning mechanisms for this problem. Specifically, for similarity measurement between the query set and each gallery set, [54] model the query set and the whole training dictionary as a convex hull to define the collaborative representation-based set-to-sets distance for classification. Hence, [54] has two characteristics: 1) the distinctiveness of the images in the query set has been exploited; 2) the feature learning and classification process is implemented in the Euclidean space. Different from [54], our approach first model the original training and test image sets onto the SPD manifold for the purpose of mining the nonlinear geometrical structural information of the data. In order to perform similarity measurement and classification, we offer two tactics. One is to map the SPD manifold-valued features into the tangent space, another is to transform them into RKHS. In these two scenarios, the Euclidean collaborative representation framework can be naturally applied. However, the proposed method does not consider the distinctiveness of the instances in the query set in the representation learning process. The aforementioned differences also leads to the different objective functions among them. Besides, the proposed approach is evaluated on four different visual classification tasks, while [54] is limited to face recognition task.

V. EXPERIMENTS AND ANALYSIS

We test the classification performance of our method on four typical visual tasks: object categorization, face recognition, virus cell classification and dynamic scene classification. For the task of set-based object categorization, we use the ETH-80 dataset [55]. The widely used YouTube Celebrities (YTC) dataset [32] is applied to the face recognition task. We utilize the MDSO dataset [56] for the task of video-based dynamic scene classification and Virus [57] for virus cell classification task.

A. Datasets and settings

The ETH-80 dataset consists of 8 categories, such as apples, cows, cups, dogs, horses, pears, tomatoes and cars, with each category has 10 image sets, and each image set contains 41 images of different perspectives. We randomly select five from each category for training and the remaining five for testing. The top line of Fig. 2 shows some examples of this dataset.

The Virus dataset is composed of 15 categories, each of which consists of 5 image sets. There are 20 different images in each set. For this dataset, 3 image sets are randomly chosen for training and the rest 2 image sets are used for testing. Some examples of Virus dataset are presented in the second line of Fig. 2.

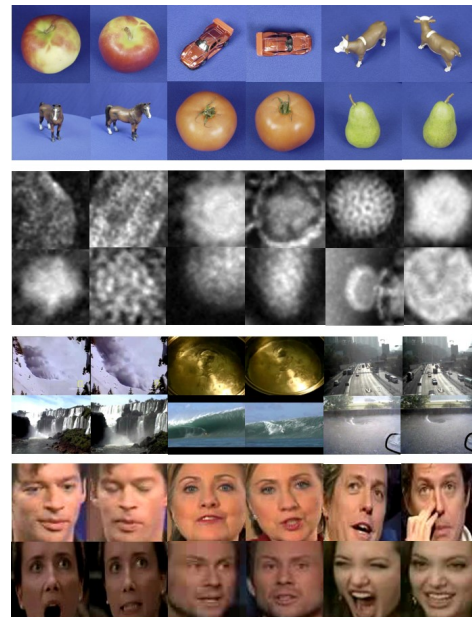


Fig. 2: Examples in four datasets. Top line: ETH-80. The second line: Virus. The third line: MDSO. Bottom line: YTC.

The MDSO dataset contains 13 different categories of dynamic scenes, with each class consists of 10 video sequences collected in an unconstrained setting. We randomly select 7 videos for training and the rest for testing in each class. As presented in the third line of Fig. 2, there are some sample images of this dataset.

For the YouTube Celebrities dataset, there are 1910 video clips of 47 subjects involved in it. Each clip consists of hundreds of face frames. We randomly choose 9 video clips in each subject with 3 for training and 6 for testing. Some sample face frames of this dataset are shown in the bottom line of Fig. 2.

To keep consistent with the previous works [32] [23] [16] [45] [47], we conduct ten-fold cross-validation experiments, i.e., repeat the randomly selecting process of the gallery/probes ten times. Then, the average classification scores are reported for each method on the four used datasets. Besides, we resize each given image into a 20×20 grayscale one.

B. Comparative methods

In order to study the effectiveness of the proposed method, we compare the proposed method with some representative image set classification methods including: Covariance Discriminant Learning (CDL) [32], Grassmann Discriminant Analysis (GDA) [35], Projection Metric Learning (PML) [36], Log-Euclidean Metric Learning (LEML) [16], Multiple Manifolds Metric Learning (MMML) [23], SPD Manifold Learning (SPDML-AIRM, SPDML-Stein) [33], Generalized Dictionary Learning and Sparse Coding using Frobenius Norm (Frob_SRC) [46], Logarithm Mapping for Sparse Representation (Log_SRC) [45], and Log-Euclidean Kernels for Sparse Representation (LogEK_SRC) [47]

We should emphasize that we use the source codes of all the comparative methods provided by the original authors

TABLE I: Average recognition rates and standard deviations of different methods on ETH-80 [55], Virus [57], MDS [56] and YTC [32] datasets.

Method	ETH-80 [55]	Virus [57]	MDS [56]	YTC [32]
CDL [32]	93.75±3.43	48.33±3.60	30.51±2.82	68.72±2.96
GDA [35]	93.25±4.80	47.00±2.49	30.51±7.78	65.78±3.34
PML [36]	90.00±3.53	47.33±3.43	29.32±4.66	67.62±3.32
LEML [16]	92.25±3.19	55.67±9.94	29.74±3.89	69.04±3.84
MMML [23]	95.00±1.89	51.13±7.67	31.95±6.26	76.70±2.81
SPDML-AIRM [33]	91.65±3.34	52.33±8.42	21.21±5.06	64.66±2.92
SPDML-Stein [33]	90.83±3.62	51.60±8.10	21.79±4.88	61.87±3.32
Frob_SRC [46]	93.25±4.43	54.75±7.83	23.75±5.67	63.16±2.72
LogEK_SRC [47]	94.88±4.17	56.33±6.37	27.95±4.94	72.55±2.77
Log_SRC [45]	95.12±4.17	55.67±7.04	34.83±5.70	74.68±2.71
LogEK_CRC	96.50±3.76	61.67±3.93	35.64±4.09	78.87±2.44
Log_CRC	97.50±1.67	64.67±5.02	36.15±5.19	78.90±2.53

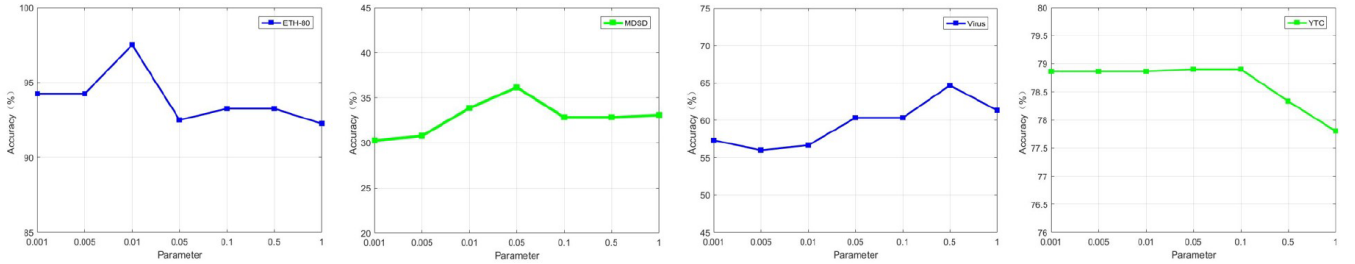


Fig. 3: The effect of regularization parameter λ_1 on accuracy for Log_CRC method.

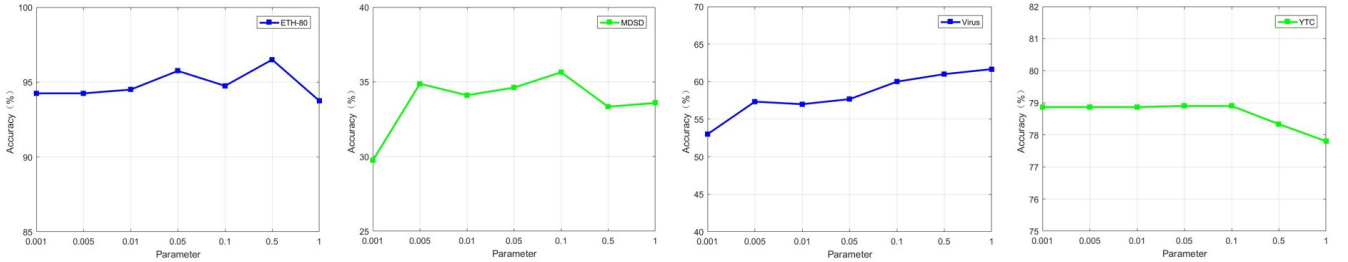


Fig. 4: The effect of regularization parameter λ_2 on accuracy for LogEK_CRC method.

to conduct experiments on the four datasets. For CDL, the perturbation is set to $10^{-3} \times \text{trace}(X)$. For GDA, the number of basis vectors for the subspace are determined by cross-validation. In PML, the number of iterations, the trade-off coefficient α and the target dimensionality d are reported according to the original work. In LEMML, the parameter η is tuned in the range of $[0.1, 1, 10]$, ζ is tuned from 0.1 to 0.5. For SPDML, following the original work [33], v_w is fixed as the minimum number of samples in one class while the dimensionality of the target SPD manifold is tuned by cross-validation. For LogEK_SRC, we use Riemannian kernel function in Eq.(4).

C. Result and Analysis

Table I lists the recognition rates of different comparative methods on the four datasets. Among them, we can intuitively see that our method, especially Log_CRC, exhibits better performance in terms of recognition scores on the four datasets. It is also interesting to see that the recognition rates of PML are lower than that of LEMML. The main difference of them is that PML conducts the projection metric learning on the Grassmann manifold, while LEMML learns the Log-Euclidean Metric on the SPD manifold, which justifies the superiority of LEM-based SPD manifold dimensionality reduction. The classification performance comparison between SPDML-Stein and SPDML-AIRM further verifies the effectiveness of the LEM-based Riemannian metric learning frameworks for image set classification. Obviously, MMML performs better than

TABLE II: The average classification scores of the different methods on the ETH-80, Virus, MDSB, and YTC datasets.

Method	ETH-80	Virus	MDSB	YTC
LogEK_CRC	96.50±3.76	61.67±3.93	35.64±4.09	78.87±2.44
Log_CRC	97.50±1.67	64.67±5.02	36.15±5.19	78.90±2.53
CRC	91.05±3.94	24.67±2.81	32.05±6.86	63.69±3.61
SPD_CRC	95.50±2.84	40.00±6.85	34.62±5.13	64.96±2.89

other competitors on the ETH-80, MDSB, and YTC datasets, because of the complementarity of multiple Riemannian manifolds is qualified to mine more powerful structural information for improved classification.

Secondly, compared with the sparse representation methods Frob_SRC, Log_SRC, LogEK_SRC and collaborative representation methods Log_CRC, LogEK_CRC, we can find that collaborative representation-based classification in tangent space and Riemannian kernel space for SPD matrix perform better than sparse representation-based classification. This could demonstrate that the collaborative representation is more efficient than L_1 -norm based sparse constraint.

Due to the regularization parameters λ_1 and λ_2 play a pivotal role in our method, we utilize cross-validation to choose suitable values for them on the four used datasets. Fig. 3 and Fig. 4 illustrate their impact on the classification results of Log_CRC and LogEK_CRC. According to these two figures, the best value of λ_1 on the ETH-80, Virus, MDSB and YTC datasets are set to 0.01, 0.5, 0.05, and 0.1, respectively. For λ_2 , 0.5, 1, 0.1, and 0.05 are the selected proper values for the ETH-80, Virus, MDSB, and YTC datasets, respectively.

TABLE III: Testing time(s) comparison of five methods on ETH-80 dataset.(For classifying one image set.)

Method	ETH-80 [55]
Frob_SRC [46]	0.212
LogEK_SRC [47]	0.147
Log_SRC [45]	0.259
LogEK_CRC	0.127
Log_CRC	0.078

D. Ablation Study for Each Component of the Proposed Framework

Although the effectiveness of the proposed approach has been demonstrated, to validate the contribution of each component of the proposed framework is also highly appealing. To this end, we make a comparison between LogEK_CRC, Log_CRC, CRC, and SPD_CRC on the ETH-80, Virus, MDSB, and YTC datasets to observe their difference in classification performance. Here, 'CRC' represents that we directly exploit the Euclidean collaborative representation to perform feature selection and classification for the original image set samples. For 'SPD_CRC', it first models the original set data onto the SPD manifold, then makes use of the Euclidean collaborative representation to conduct feature learning and classification in this space. The final classification results of them are listed in Table II. According to this table, it is evident that the classification accuracies of CRC are

significantly lower than that of other three competitors on the four used datasets. The reason may be that the original image set samples contain large within-class variational information, which restrains CRC from mining more pivotal information for classification. After modeling these data onto the SPD manifold, the classification ability of SPD_CRC has been further promoted compared to CRC, which confirms the effectiveness of Riemannian manifold in mining the nonlinear geometrical structure of the visual data. However, an obvious limitation of SPD_CRC is the Euclidean collaborative representation-based classification is directly carried out on the SPD manifold, which inevitably leads to the sub-optimal solution. From Table II, it is also worth noting that the proposed LogEK_CRC and Log_CRC outperform SPD_CRC and CRC in terms of classification score on the four used datasets, visibly. These experimental observations demonstrate the significance of each module of the proposed framework for image set classification.

E. Testing Time Comparison

Table III presents the testing time of the proposed methods and several sparse representation methods on the ETH-80 dataset. The experiments were run on 3.0GHz PC with 4GB RAM and Matlab2016a software. We need to emphasize that the testing time is computed by classifying one test sample with the whole gallery. From Table III, it is clear to see that the testing burden of the proposed Log_CRC and LogEK_CRC has been reduced compared to other competitors. The reasons are twofold: 1) our method classifies the query set with the gallery directly instead of classifying by learning a dictionary in SRC methods; 2) our method has closed-form analytical solutions.

VI. CONCLUSION

This paper proposes a collaborative representation-based image set classification algorithm in the context of SPD manifold. For this approach, we suggest two ways to implement feature extraction and classification, one is to map the SPD manifold-valued data representations into the tangent space via matrix logarithm map, another is to embed them into RKHS using the Riemannian kernel function. After that, the merits of Euclidean collaborative representation are qualified to be generalised to the SPD manifold.

Experimental results obtained on four different benchmarking datasets show that the proposed approach could make a considerable improvement in classification performance and computational efficiency compared to some representative image set classification methods. For future work, we plan to integrate dictionary learning into the proposed framework for further improving the discriminability of the learned geometric features.

REFERENCES

- [1] Lei Zhang, Meng Yang, and Xiangchu Feng. Sparse representation or collaborative representation: Which helps face recognition? In *2011 International conference on computer vision*, pages 471–478. IEEE, 2011.

- [2] Meng Yang, Lei Zhang, Xiangchu Feng, and David Zhang. Fisher discrimination dictionary learning for sparse representation. In *2011 International Conference on Computer Vision*, pages 543–550. IEEE, 2011.
- [3] Hui Li, Xiao-Jun Wu, and Tariq Durrani. Nestfuse: An infrared and visible image fusion architecture based on nest connection and spatial/channel attention models. *IEEE Transactions on Instrumentation and Measurement*, 69(12):9645–9656, 2020.
- [4] Hui Li and Xiao-Jun Wu. Multi-focus image fusion using dictionary learning and low-rank representation. *International Conference on Image and Graphics*, pages 675–686, 2017.
- [5] Xiaoqing Luo, Zhancheng Zhang, Baocheng Zhang, and Xiao-Jun Wu. Image fusion with contextual statistical similarity and nonsubsampling shearlet transform. *IEEE Sensors Journal*, 17(6):1760–1771, 2017.
- [6] C Li, W Yuan, AC Bovik, and X Wu. No-reference blur index using blur comparisons. *Electronics letters*, 47(17):962–963, 2011.
- [7] Qingbing Sang, Huixin Qi, Xiaojun Wu, Chaofeng Li, and Alan C Bovik. No-reference image blur index based on singular value curve. *Journal of Visual Communication and Image Representation*, 25(7):1625–1630, 2014.
- [8] Matej Kristan, Aleš Leonardis, Jiří Matas, Michael Felsberg, Roman Pflugfelder, Joni-Kristian Kämäräinen, Martin Danelljan, Luka Čehovin Zajc, Alan Lukežič, Ondrej Dřbohlav, et al. The eighth visual object tracking vot2020 challenge results. *European Conference on Computer Vision*, pages 547–601, 2020.
- [9] Jun Sun, Chao Li, Xiao-Jun Wu, Vasile Palade, and Wei Fang. An effective method of weld defect detection and classification based on machine vision. *IEEE Transactions on Industrial Informatics*, 15(12):6322–6333, 2019.
- [10] Lishan Qiao, Songcan Chen, and Xiaoyang Tan. Sparsity preserving projections with applications to face recognition. *Pattern Recognition*, 43(1):331–341, 2010.
- [11] Li Zhang, Wei-Da Zhou, Pei-Chann Chang, Jing Liu, Zhe Yan, Ting Wang, and Fan-Zhang Li. Kernel sparse representation-based classifier. *IEEE Transactions on Signal Processing*, 60(4):1684–1695, 2012.
- [12] Zhang Lei, Yang Meng, and Xiangchu Feng. Sparse representation or collaborative representation: Which helps face recognition? In *International Conference on Computer Vision*, 2011.
- [13] Lei Zhang, Meng Yang, Xiangchu Feng, Yi Ma, and David Zhang. Collaborative representation based classification for face recognition. *arXiv preprint arXiv:1204.2358*, 2012.
- [14] Wei Li and Qian Du. Joint within-class collaborative representation for hyperspectral image classification. *IEEE Journal of Selected Topics in Applied Earth Observations and Remote Sensing*, 7(6):2200–2208, 2014.
- [15] Sijia Cai, Lei Zhang, Wangmeng Zuo, and Xiangchu Feng. A probabilistic collaborative representation based approach for pattern classification. In *Proceedings of the IEEE conference on computer vision and pattern recognition*, pages 2950–2959, 2016.
- [16] Zhiwu Huang, Ruiping Wang, Shiguang Shan, Xianqiu Li, and Xilin Chen. Log-euclidean metric learning on symmetric positive definite manifold with application to image set classification. In *International conference on machine learning*, pages 720–729, 2015.
- [17] Kai-Xuan Chen and Xiao-Jun Wu. Component spd matrices: A low-dimensional discriminative data descriptor for image set classification. *Computational Visual Media*, 4(3):245–252, 2018.
- [18] Zifeng Wu, Yongzhen Huang, and Liang Wang. Learning representative deep features for image set analysis. *IEEE Transactions on Multimedia*, 17(11):1960–1968, 2015.
- [19] Kai-Xuan Chen, Xiao-Jun Wu, Rui Wang, and Josef Kittler. Riemannian kernel based nyström method for approximate infinite-dimensional covariance descriptors with application to image set classification. In *2018 24th International Conference on Pattern Recognition (ICPR)*, pages 651–656. IEEE, 2018.
- [20] Gong Cheng, Peicheng Zhou, and Junwei Han. Duplex metric learning for image set classification. *IEEE Transactions on Image Processing*, 27(1):281–292, 2017.
- [21] Rui Wang, Xiao-Jun Wu, and Josef Kittler. Symnet: A simple symmetric positive definite manifold deep learning method for image set classification. *IEEE Transactions on Neural Networks and Learning Systems*, pages 1–15, 2021.
- [22] Wen Wang, Ruiping Wang, Shiguang Shan, and Xilin Chen. Discriminative covariance oriented representation learning for face recognition with image sets. In *Proceedings of the IEEE Conference on Computer Vision and Pattern Recognition*, pages 5599–5608, 2017.
- [23] Rui Wang, Xiao-Jun Wu, Kai-Xuan Chen, and Josef Kittler. Multiple manifolds metric learning with application to image set classification. In *2018 24th International Conference on Pattern Recognition (ICPR)*, pages 627–632. IEEE, 2018.
- [24] Rui Wang, Xiao-Jun Wu, Kai-Xuan Chen, and Josef Kittler. Multiple riemannian manifold-valued descriptors based image set classification with multi-kernel metric learning. *IEEE Transactions on Big Data*, 2020.
- [25] Rui Wang, Xiao-Jun Wu, Zhen Liu, and Josef Kittler. Geometry-aware graph embedding projection metric learning for image set classification. *IEEE Transactions on Cognitive and Developmental Systems*, pages 1–1, 2021.
- [26] Xiao-Jun Wu, Josef Kittler, Jing-Yu Yang, Messer Kieron, and Shitong Wang. A new direct lda (d-lda) algorithm for feature extraction in face recognition. *Proceedings of the 17th International Conference on Pattern Recognition*, 4:545–548, 2004.
- [27] Y-J Zheng, J-Y Yang, Jian Yang, X-J Wu, and Z Jin. Nearest neighbour line nonparametric discriminant analysis for feature extraction. *Electronics Letters*, 42(12):679–680, 2006.
- [28] Su-Gen Chen and Xiao-Jun Wu. A new fuzzy twin support vector machine for pattern classification. *International Journal of Machine Learning and Cybernetics*, 9(9):1553–1564, 2018.
- [29] Guan-Lin Shen and Xiao-Jun Wu. Content based image retrieval by combining color, texture and centrality. *2013 Constantinides International Workshop on Signal Processing*, pages 16–16, 2013.
- [30] Xiaoqing Luo, Zhancheng Zhang, and Xiaojun Wu. A novel algorithm of remote sensing image fusion based on shift-invariant shearlet transform and regional selection. *AEU-International Journal of Electronics and Communications*, 70(2):186–197, 2016.
- [31] Zhen-Hua Feng, Josef Kittler, Muhammad Awais, Patrik Huber, and Xiao-Jun Wu. Face detection, bounding box aggregation and pose estimation for robust facial landmark localisation in the wild. *Proceedings of the IEEE conference on computer vision and pattern recognition workshops*, pages 160–169, 2017.
- [32] Ruiping Wang, Huimin Guo, Larry S Davis, and Qionghai Dai. Covariance discriminative learning: A natural and efficient approach to image set classification. In *Computer Vision and Pattern Recognition (CVPR), 2012 IEEE Conference on*, pages 2496–2503. IEEE, 2012.
- [33] Mehrtash T Harandi, Mathieu Salzmann, and Richard Hartley. From manifold to manifold: Geometry-aware dimensionality reduction for spd matrices. In *European conference on computer vision*, pages 17–32. Springer, 2014.
- [34] Mehrtash Harandi, Mathieu Salzmann, and Richard Hartley. Dimensionality reduction on spd manifolds: The emergence of geometry-aware methods. *IEEE transactions on pattern analysis and machine intelligence*, 40(1):48–62, 2018.
- [35] Jihun Hamm and Daniel D Lee. Grassmann discriminant analysis: a unifying view on subspace-based learning. In *Proceedings of the 25th international conference on Machine learning*, pages 376–383. ACM, 2008.
- [36] Zhiwu Huang, Ruiping Wang, Shiguang Shan, and Xilin Chen. Projection metric learning on grassmann manifold with application to video based face recognition. In *Proceedings of the IEEE conference on computer vision and pattern recognition*, pages 140–149, 2015.
- [37] Rui Wang, Xiao-Jun Wu, and Josef Kittler. Graph embedding multi-kernel metric learning for image set classification with grassmannian manifold-valued features. *IEEE Transactions on Multimedia*, 23:228–242, 2020.
- [38] Wen Wang, Ruiping Wang, Zhiwu Huang, Shiguang Shan, and Xilin Chen. Discriminant analysis on riemannian manifold of gaussian distributions for face recognition with image sets. In *Proceedings of the IEEE conference on computer vision and pattern recognition*, pages 2048–2057, 2015.
- [39] Vincent Arsigny, Pierre Fillard, Xavier Pennec, and Nicholas Ayache. Geometric means in a novel vector space structure on symmetric positive-definite matrices. *SIAM journal on matrix analysis and applications*, 29(1):328–347, 2007.
- [40] Xavier Pennec, Pierre Fillard, and Nicholas Ayache. A riemannian framework for tensor computing. *International Journal of computer vision*, 66(1):41–66, 2006.
- [41] Yu-jie Zheng, Jian Yang, Jing-yu Yang, and Xiao-jun Wu. A reformative kernel fisher discriminant algorithm and its application to face recognition. *Neurocomputing*, 69(13-15):1806–1810, 2006.
- [42] Mehrtash T Harandi, Conrad Sanderson, Richard Hartley, and Brian C Lovell. Sparse coding and dictionary learning for symmetric positive definite matrices: A kernel approach. In *European Conference on Computer Vision*, pages 216–229. Springer, 2012.
- [43] Sadeep Jayasumana, Richard Hartley, Mathieu Salzmann, Hongdong Li, and Mehrtash Harandi. Kernel methods on the riemannian manifold of symmetric positive definite matrices. In *Proceedings of the IEEE*

- Conference on Computer Vision and Pattern Recognition*, pages 73–80, 2013.
- [44] Zhiwu Huang, Ruiping Wang, Shiguang Shan, and Xilin Chen. Face recognition on large-scale video in the wild with hybrid euclidean-and-riemannian metric learning. *Pattern Recognition*, 48(10):3113–3124, 2015.
- [45] Guo Kai, Prakash Ishwar, and Janusz Konrad. Action recognition using sparse representation on covariance manifolds of optical flow. In *IEEE International Conference on Advanced Video & Signal Based Surveillance*, 2010.
- [46] Suvrit Sra and Anoop Cherian. Generalized dictionary learning for symmetric positive definite matrices with application to nearest neighbor retrieval. In *Joint European Conference on Machine Learning and Knowledge Discovery in Databases*, pages 318–332. Springer, 2011.
- [47] Peihua Li, Qilong Wang, Wangmeng Zuo, and Lei Zhang. Log-euclidean kernels for sparse representation and dictionary learning. In *Proceedings of the IEEE International Conference on Computer Vision*, pages 1601–1608, 2013.
- [48] Mehrtash T Harandi, Richard Hartley, Brian Lovell, and Conrad Sander-son. Sparse coding on symmetric positive definite manifolds using bregman divergences. *IEEE transactions on neural networks and learning systems*, 27(6):1294–1306, 2016.
- [49] Vincent Arsigny, Pierre Fillard, Xavier Pennec, and Nicholas Ayache. Log-euclidean metrics for fast and simple calculus on diffusion tensors. *Magnetic Resonance in Medicine: An Official Journal of the International Society for Magnetic Resonance in Medicine*, 56(2):411–421, 2006.
- [50] Biao Wang, Weifeng Li, Norman Poh, and Qingmin Liao. Kernel collaborative representation-based classifier for face recognition. In *2013 IEEE International Conference on Acoustics, Speech and Signal Processing*, pages 2877–2881. IEEE, 2013.
- [51] Shenghua Gao, Ivor Wai-Hung Tsang, and Liang-Tien Chia. Sparse representation with kernels. *IEEE Transactions on Image Processing*, 22(2):423–434, 2012.
- [52] Yuwei Wu, Yunde Jia, Peihua Li, Jian Zhang, and Junsong Yuan. Manifold kernel sparse representation of symmetric positive-definite matrices and its applications. *IEEE Transactions on Image Processing*, 24(11):3729–3741, 2015.
- [53] Dong Wei, Xiaobo Shen, Quansen Sun, Xizhan Gao, and Wenzhu Yan. Prototype learning and collaborative representation using grassmann manifolds for image set classification. *Pattern Recognition*, 100:107123, 2020.
- [54] Pengfei Zhu, Wangmeng Zuo, Lei Zhang, Simon Chi-Keung Shiu, and David Zhang. Image set-based collaborative representation for face recognition. *IEEE transactions on information forensics and security*, 9(7):1120–1132, 2014.
- [55] Bastian Leibe and Bernt Schiele. Analyzing appearance and contour based methods for object categorization. In *Computer Vision and Pattern Recognition, 2003. Proceedings. 2003 IEEE Computer Society Conference on*, volume 2, pages II–409. IEEE, 2003.
- [56] Nitesh Shroff, Pavan Turaga, and Rama Chellappa. Moving vistas: Exploiting motion for describing scenes. In *Computer Vision and Pattern Recognition (CVPR), 2010 IEEE Conference on*, pages 1911–1918. IEEE, 2010.
- [57] Gustaf Kylberg, Mats Uppström, and Ida-Maria Sintorn. Virus texture analysis using local binary patterns and radial density profiles. In *Iberoamerican Congress on Pattern Recognition*, pages 573–580. Springer, 2011.